Analytical Methods

ROYAL SOCIETY OF CHEMISTRY

CRITICAL REVIEW

View Article Online
View Journal | View Issue

Check for updates

Cite this: *Anal. Methods*, 2025, **17**, 4496

A gold nanoparticle-based colorimetric strategy for DNA detection: principles and novel approaches

Nguyen Tran Truc Phuong, †[a] Hanh An Nguyen, †[b] Thi Ngoc Diep Trinh *[c] and Kieu The Loan Trinh ‡*[d]

The development of nanotechnology has led to the rapid growth of many different fields, including sensors. Bulky and complex sensor systems are gradually being replaced by streamlined sensor devices with advantages in size, simplicity, cost-effectiveness, and fast response, allowing qualitative detection of target analyte on-site application for clinical diagnosis. Significantly, since the COVID-19 pandemic, research on developing test kits for detecting biological molecules has grown rapidly, with an increasing number of publications. The number of studies developing colorimetric sensors based on gold nanoparticles (AuNPs) has increased continuously over the years, demonstrating the potential application of this material. The surface plasmon resonance (SPR) effect and high biocompatibility of AuNPs make them different from many other metal nanomaterials. In addition, the peroxidase activity properties of AuNPs have also received much attention in colorimetric sensors. In this review, the colorimetric sensors developed based on the AuNP material platform for DNA detection will be discussed in detail. Among them, the commonly used synthesis methods of AuNPs based on their applications and the primary mechanism of AuNP-based colorimetric sensors for DNA detection will be discussed. In addition, AuNP-based colorimetric applications in POCT for pathogenic bacteria and viruses are also mentioned in this review to provide a broader perspective on the potential and developmental direction of AuNP-based colorimetric sensors. Another aspect this review provides is development strategies that allow simple readout using the naked eye, a spectrophotometer, or a smartphone camera, which present many opportunities for integration into other electronic devices.

Received 28th January 2025
Accepted 1st May 2025

DOI: 10.1039/d5ay00148j

rsc.li/methods

Published on 02 maggio 2025. Downloaded on 14/02/2026 03:50:09.

Introduction

In recent years, colorimetric sensors have emerged as a trend and have been widely developed for detecting various analytes such as antibiotics,[1] metals,[2] organic pollutants,[3] and even biological molecules such as proteins,[4] DNA,[5] RNA,[6] bacteria,[7] or viruses.[8] The aim of manufacturing simple, compact, fast-response on-site sensor chips for clinical diagnosis is to gradually replace bulky sensor systems. The transducer, processing unit, and detection unit are gradually streamlined to create compact and convenient sensor devices. Reading results becomes simpler through color, which does not require the support of signal converters and analysis experts. The general mechanism of colorimetric sensors is mainly based on the interaction of the target analyte with the detector, which causes color changes that allow the qualitative identification of the target analyte. The color signal can come from the change in optical properties of the probe material, usually the surface plasmon resonance (SPR) effect of metal nanoparticles such as Au, Ag, Cu, and Ni.[9–11] The SPR effect is characterized by a sensitive change in the resonance frequency to changes under dielectric conditions.[12,13] Consequently, the electrostatic interaction of biomolecules with the probe material is sensitively detected by a color change.

With the continuous development of nanotechnology, gold nanoparticles (AuNPs) are increasingly showing great potential in many different fields, notably in sensors.[14] Many advantages of AuNPs, such as a high surface area to volume ratio, stability, biocompatibility, versatile surface chemistry amenable to functionalization, and unique optical and electrical properties, have been demonstrated in many previous publications.[15,16] Among them, SPR and peroxidase activity are the keys that make gold nanoparticles attractive in point-of-care testing (POCT) sensors based on colorimetric methods. The size effect of AuNPs plays an important role in the development of

[a]*NTT Hi-Tech Institute, Nguyen Tat Thanh University, Ward 13, District 04, Ho Chi Minh City 70000, Vietnam*

[b]*Department of Molecular Biology, Institute of Food and Biotechnology, Can Tho University, Can Tho City 94000, Vietnam*

[c]*BioTechnology Institute, Tra Vinh University, Tra Vinh City 87000, Vietnam. E-mail: ttndiep@tvu.edu.vn*

[d]*Bionano Applications Research Center, Gachon University, 1342 Seongnam-daero, Sujeong-gu, Seongnam-si, Gyeonggi-do, 13120, Korea. E-mail: tktloan@gmail.com*

† These authors contributed equally to this work.

‡ Current address: Center for Innovative Materials and Architectures, Viet Nam National University, Ho Chi Minh City 70000, Vietnam.

This journal is © The Royal Society of Chemistry 2025

Published on 02 maggio 2025. Downloaded on 14/02/2026 03:50:09.

colorimetric sensors. Wrigglesworth *et al.* experimentally demonstrated the influence of size on the absorption and scattering rates of AuNPs which was predicted by the Mie theory of the optical resonance wavelength of spherical nanoparticles.[17] On the other hand, the morphology and dispersion of AuNPs also cause many sensitive changes in the plasmon resonance frequency of gold nanoparticles, leading to the diversity of sensing mechanisms using AuNP probes. The AuNPs can be synthesized using various methods that meet the quality requirements of each application field. Compared with AgNPs, AuNPs show much higher stability and biocompatibility, which are particularly interesting in biosensors.[18,19] In addition, AuNPs showed better interaction with thiol and amine groups than AgNPs, which showed that AuNPs' high interaction with analytes is suitable for colorimetric sensor applications. On the other hand, AuNPs also show outstanding advantages in developing colorimetric sensors based on catalytic mechanisms. Bohdanovych *et al.* demonstrated that the catalytic decolorization of methylene blue by AuNPs was significantly superior to that of AgNPs when *A. annua* hairy root extracts were used in the biosynthesis.[20] Therefore, AuNPs become the preferred choice for color-based sensing applications derived from the SPR effect compared to other metal nanoparticles such as Ag, Cu, or Ni.

Publications per year (from January 2001 to January 2025) with keywords "Gold nanoparticles/Colorimetric" observed from the chart in Fig. 1a show the rapid and continuous increase in publications from 2001 to 2018 and the stability of the number of publications per year from 2019 to 2024 reflecting the achievements and importance of colorimetric AuNP-based sensors. In the last five years, from 2021–2025, there were more than 2360 publications accounting for 29.84% of the total number of publications related to the keyword "Gold nanoparticles/Colorimetric" based on the Web of Science, showing the heat of this topic for the needs of the radiology society. The impacts of the COVID-19 pandemic show the importance of accurate, intuitive, instantaneous, accessible, and cost-effective biomolecule detection sensors. False positive results cause many difficulties in isolation, treatment, control, and tracing the origin of an epidemic.[21–23] Therefore, accuracy is one factor that must be focused on color-based sensors. Fig. 1b shows the total number of publications when searching with the keyword "Gold nanoparticles/Colorimetric" combined with the keyword DNA compared to when combined with keywords such as RNA, battery, and virus based on the Web of Science in the last five years. DNA can be used as an aptamer to create a sensitive and selective detection platform for target molecules or targets due to its high specificity and good binding ability to

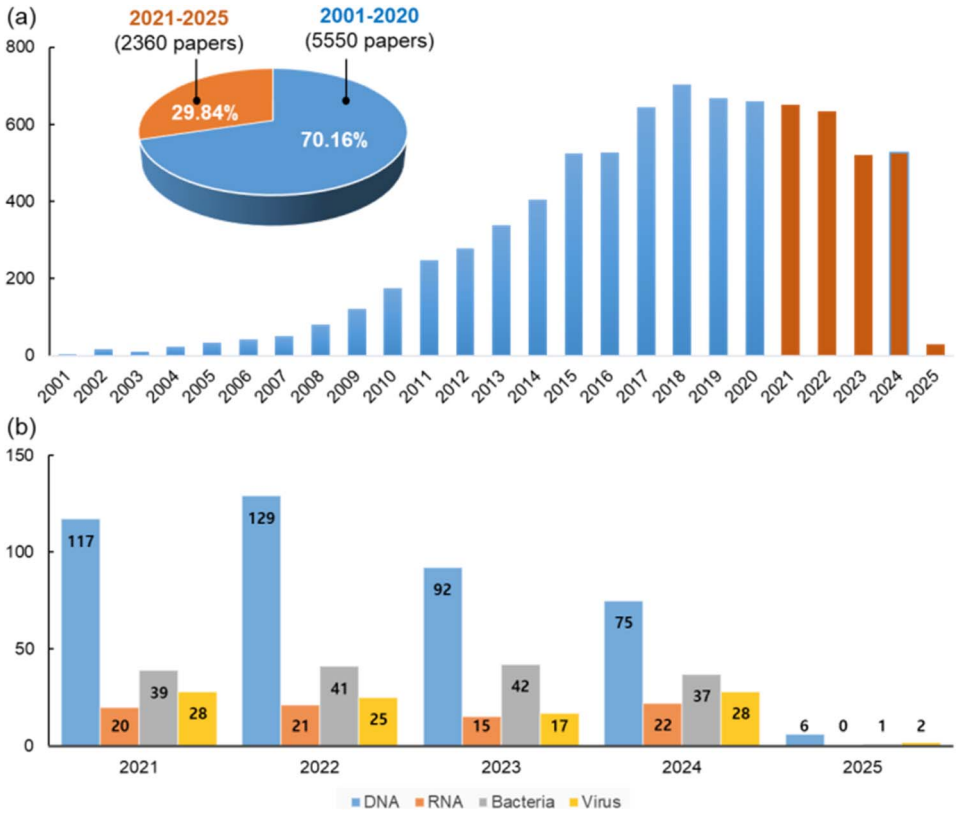

Fig. 1 (a) The chart shows the total number of publications per year (from January 2001 to January 2025) with keywords "Gold nanoparticles/Colorimetric". (b) The chart shows the total number of publications in the last 5 years (from 2021 to 2025) with keywords "Gold nanoparticles/Colorimetric/DNA", "Gold nanoparticles/Colorimetric/RNA", "Gold nanoparticles/Colorimetric/Bacteria", and "Gold nanoparticles/Colorimetric/Virus". The results are based on the Web of Science (WoS; https://www.webofscience.com) database. The search was updated on January 14th, 2023.

Published on 02 maggio 2025. Downloaded on 14/02/2026 03:50:09.

metal nanoparticles based on electrostatic interactions. Additionally, the DNA sensor can detect and identify species in complex samples without undergoing an extraction process.[24]

This review discusses the development strategies of colorimetric sensors for DNA detection applications based on AuNP material platforms. In general, colorimetric sensor probes, although developed in various ways, mainly focus on exploiting two outstanding properties of AuNPs: SPR and peroxidase activity. Specifically, the SPR-based color change mechanisms, including aggregation, dispersion, growth-mediated, and accumulation-based methods, and peroxidase-based methods, are discussed in detail. Besides, the commonly used methods and the recently developed trends in the fabrication and property control of AuNPs are considered in the review. Finally, an extensive evaluation showing the potential of AuNP-based colorimetric sensors for POCT applications for bacterial and viral detection was performed.

Synthesis of gold nanoparticles for colorimetric DNA sensors

Chemical reduction method

Chemical reduction is one of the simplest and most commonly used methods for the synthesis of AuNPs. Various reduction-based synthesis methods have been developed such as the Turkevich method,[25] synthesis with $NaBH_4$ with/without citrate,[26] seeding-growth,[27] synthesis by ascorbic acid,[28] green synthesis,[29] Brust–Schiffrin method,[30] and synthesis using other reducing agents.[31,32] In general, all of them are based on the properties of chemical reduction reactions with the formation of gold nanoparticles typically occurring in three stages: reduction, nucleation, and growth, usually starting from gold salts, commonly gold(III) chloride hydrate. Initially, Au^0 atoms are generated from reducing Au^{3+} ions and cluster together to form seed particles. These seeds then develop into gold nanoparticles, which are dispersed in solution with the support of surface stabilizers. A reducing agent is crucial for the formation of AuNPs, as it influences the reaction rate and subsequently affects the particle size.[33–35] The morphology of AuNPs is significantly affected by the reducing, napping, and stabilizing agents. By controlling the reaction rate and using appropriate capping agents, the growth of AuNPs can be directed toward desired crystallographic orientations (Fig. 2). Personick *et al.* used a seed-mediated method to successfully synthesize two {110}-faceted gold nanostructure-rhombic dodecahedra and obtuse triangular bipyramids based on the synergistic effect of low concentrations of Ag^+ and Cl^- in the surfactant (cetyltrimethylammonium chloride (CTAC)) as a stabilizer.[37] The interactions of surface stabilizers can significantly affect the growth of lattice planes during synthesis. The bromide ion (Br^-) in cetyltrimethylammonium bromide (CTAB) exhibits a stronger binding affinity to the gold surface compared to the chloride ion (Cl^-) in CTAC. As a result, the presence of Br^- reduces the predominance of silver (Ag) on the {110} face of Au, leading to less uniform particle formation than when CTAC is used as the surface stabilizer. In addition, the synthesis conditions, such as temperature, reaction time, pH, *etc.*, significantly affect the morphology and size of AuNPs. Yazdani *et al.* conducted a study to evaluate the influence of pH and reaction time on the Turkevich synthesis of AuNPs to control the size of AuNPs suitable for medical applications.[38] In this method, the concentration of trisodium citrate dihydrate alters the pH of the solution. Their investigation revealed that as the pH increased with higher concentrations of trisodium citrate

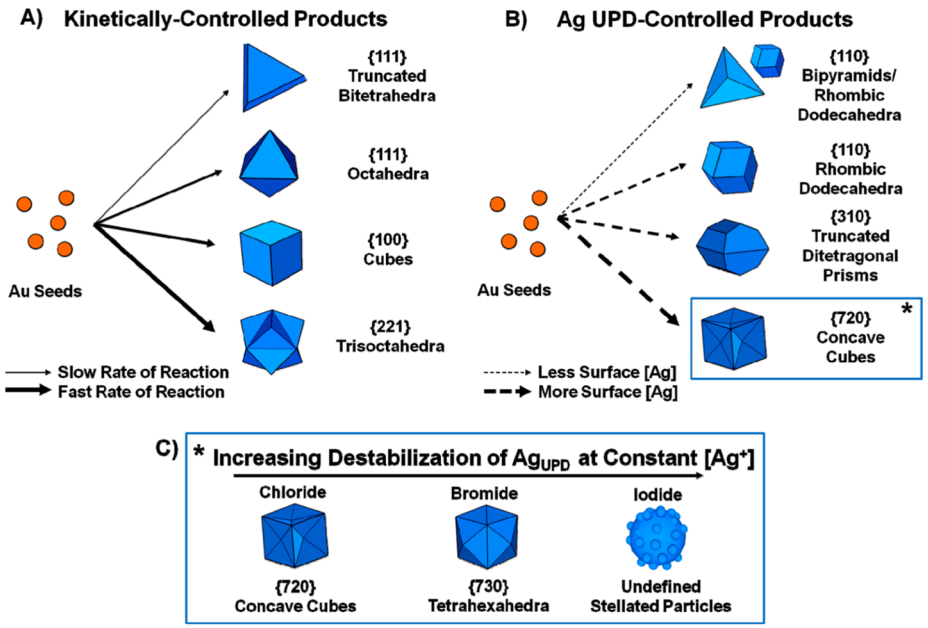

Fig. 2 Schematic diagram illustrating the growth direction of AuNPs in different shapes: (A) kinetically controlled; (B) Ag underpotential deposition-controlled products; (C) influence of Cl^-, Br^-, and I^- at high concentrations.[36]

 This journal is © The Royal Society of Chemistry 2025

Published on 02 maggio 2025. Downloaded on 14/02/2026 03:50:09.

dihydrate, the size of the AuNPs decreased. Additionally, pH also influences the monodispersity of AuNPs. The results indicated that the AuNPs were best monodispersed at a pH of at least 6, which correlated directly with the concentration of citrate in the solution. Furthermore, an increase in nanoparticle size was found to be directly proportional to the reaction time. Many studies have shown that the temperature of the synthesis process affects the speed and size of AuNPs; specifically, at low temperatures, the reduction process is slower, thus prolonging the synthesis time, and the consequence of this is an increase in particle size. Mountrichas *et al.* proposed a simple one-step synthesis of AuNPs using poly(dimethylaminoethyl methacrylate) homopolymer as both a reducing agent and stabilizer.[39] The results of the temperature investigation showed that the particles were produced with high uniformity and reaction time at high temperatures. On the other hand, solvent properties, such as polarity, boiling point, viscosity, and surface tension, play essential roles in controlling the morphology, size, structure, and stability of AuNPs.[40] He *et al.* used ethanol as an antisolvent to exchange with organic solvents such as DDAB and alkylamine (dodecylamine, hexadecylamine, and octadecylamine).[41] Ensuring the dispersion of AuNPs is of great significance in the application of AuNPs in many fields.

Electrochemical method

Electrochemical synthesis of gold nanoparticles is less used than chemical reduction, but the advantages of particle quality, stability, limited use of reducing agents, and low generation of by-products have attracted much attention from researchers for many different applications.[42] The size and morphology of AuNPs are controlled by controlling the applied voltage and the concentration of the surface stabilizer. In electrochemical methods, gold nanoparticles can be produced from gold salts or sacrificial anodes in commonly used organic solvents such as tetraalkylammonium salts, acetonitrile, polypyrrole, and poly(*N*-vinylpyrrolidone) with the participation of cationic surfactants as surface active agents. Yu *et al.* reported a technique to synthesize gold nanorods (AuNRs) by electrochemical oxidation/reduction with a gold plate ($3 \times 1 \times 0.05$ cm) as the anode electrode and a platinum plate ($3 \times 1 \times 0.05$ cm) as the cathode electrode combined with the electrolyte solution containing hexadecyltrimethylammonium bromide ($C_{16}TAB$) acting as the supporting electrolyte and a nanoparticle stabilizer.[43] A 3 mA current is maintained throughout the electrolysis process to oxidize the sacrificial anode electrode to produce Au^{3+} ions, which participate in the reduction process at the cathode electrode. Under the effect of ultrasound and surface stabilizers, the gold nanoparticles with controlled size were well-dispersed in the solution. In another research study, Liu *et al.* used a platinum rotating electrode as the cathode to reduce the deposition of AuNPs at the cathode and improve the efficiency of the electrochemical synthesis.[44] Based on the hydrolysis mechanism of poly(*N*-vinylpyrrolidone) (PVP) under acid and base catalysis locally at the anode and cathode electrodes created from the water electrolysis process to generate the products that have different reduction levels leading to the formation of different gold nanoproducts. Similarly, Haro-González *et al.* presented a method for synthesizing AuNPs in an aqueous medium in the presence of ethylene glycol as a stabilizer.[45] A −0.9 V electrostatic source was applied to the basic electrochemical system consisting of 3 electrodes (work, counter, and reference electrodes) under continuous magnetic stirring conditions to produce AuNPs from Au^{3+} ion reduction. In addition to stabilizing the AuNPs, poly(ethylene glycol) also serves as a highly biocompatible coating material, thus having potential applications in the biomedical field. Recently, plasma-driven solution electrochemistry (PDSE) has received much attention for its application in the synthesis of nanoparticles as an alternative to conventional wet electrochemical methods due to its advantages such as fast reaction time, in the absence of additional stabilizers or ligands, and increased purity of the resulting materials.[46,47] Nam *et al.* reported a rapid synthesis of stabilizer-free gold nanoparticles based on the interaction between low-temperature plasma and liquid to convert $AuCl_4^-$ to form AuNPs in a short time, with the size increasing proportionally to the droplet residence time.[48] The formation time scale and growth mechanism of AuNPs are shown in Fig. 3. When reaching the supersaturated state, the Au^0 atoms formed from the plasma treatment create Au nuclei. This process takes place in only about 10 ms and stops when the Au^0 is exhausted. The AuNPs will be formed inside the plasma droplet due to diffusion-driven monomer absorption and continue to grow to larger sizes based on the autocatalytic surface reaction after leaving the plasma droplet. Nam *et al.* continued to study the effect of pH on the formation of AuNPs using the PDSE method to propose a strategy for synthesizing and controlling the size of AuNPs.[49] The results showed that the size and size distribution of the particles tended to decrease with increasing pH, which was caused by the elongated nucleation timescale at low solution pH. Based on the principle of nucleation formation in PDSE, it is possible to adjust its timescale from autocatalytic particle growth to produce AuNPs with small size and narrow size distribution. Besides other factors, such as modulation of pulsed discharge, $AuCl_4^-$ concentration is also an effective strategy in controlling the properties of AuNPs during the synthesis process. Although there are many advantages such as reaction time, high particle purity, and uniformity, the complex formation mechanism and high requirements for specialized equipment for the fabrication process have become barriers to the widespread development of this method.

Green synthesis method from a plant extract

Along with the rapid development of nanotechnology, many issues regarding its impact on the sustainable development of the environment have been raised. Green synthesis opens a new path in the development of nanotechnology in a sustainable, environmentally friendly, and less toxic direction. To reduce the amount of chemical waste released into the environment and reduce the level of danger in synthesizing nanomaterials by chemical methods, plant extracts have been used as a substitute for reducing or stabilizing agents in fabricating nanoparticles. This method can be considered a simple and less expensive

Published on 02 maggio 2025. Downloaded on 14/02/2026 03:50:09.

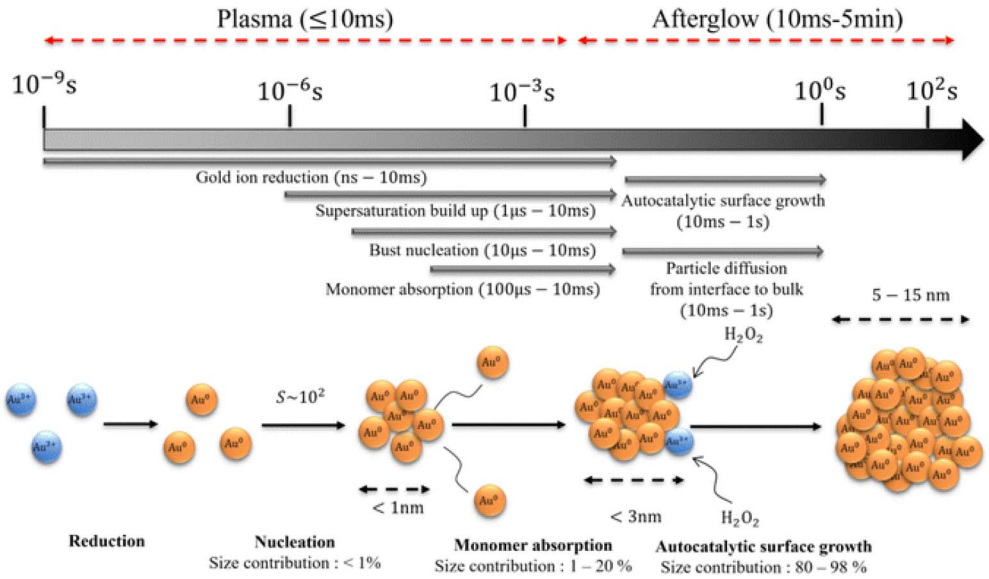

Fig. 3 Schematic of the formation mechanism of gold nanoparticles in a plasma–droplet system.[48]

green synthesis route for nanoparticles compared to some techniques that use physical agents such as UV irradiation,[50] laser ablation,[51] ultrasonic fields,[52] and photochemical reduction.[53] Natural compounds found in plants are a rich source of reducing agents and stabilizers for synthesizing nanomaterials in large quantities. Many studies on the synthesis of gold nanoparticles from plant compounds have shown high efficiency, increasing the applicability of AuNPs in the biomedical field. Stabilized or capped AuNPs with plant-derived compounds help solve problems related to cytotoxicity.[54,55] In addition, these compounds also show the ability to stabilize and control the morphology and size of AuNPs, which greatly affect their properties. Phenolic compounds commonly found in plants are rich sources of reducing agents and stabilizers for green synthesis of AuNPs. Singh *et al.* presented the general overview and mechanism involved in green synthesis of nanoparticles using extracted plants as depicted in Fig. 4a.[56] Phenolic compounds can be extracted from different parts of plants, such as leaves, stems, roots, and fruits, depending on the type of plant to obtain the highest concentration. However, the content of these substances in the plant can vary depending on the season and soil, which leads to many difficulties in maintaining uniformity in the concentration of batches. In addition, many studies have shown that green synthesized AuNPs show significantly reduced toxicity and good biodegradability compared to those synthesized using chemical-reducing agents. Eltahir *et al.* successfully synthesized AuNPs from six phenolic compounds isolated from the extract of *Glycyrrhiza glabra* including liquiritin, isoliquiritin, neoisoliquiritin, isoliquiritin apioside, liquiritin apioside, and glabridin.[58] The common feature of these materials is their strong reducing properties, which donate electrons to reduce Au^{3+} to Au^{0} rapidly, which helps to control the size of AuNPs at the nanometer level. In addition, the different interactions of phenolics during both reduction and stabilization give rise to different morphologies and sizes of nanoparticles. Typically, phenolic compounds from plant extracts act as both reducing agents and stabilizing or capping agents in the green synthesis of AuNPs. Phenolic ligands not only help control the size and limit the aggregation of AuNPs by creating interparticle repulsion but also help increase the surface activities of AuNPs. The mechanism of formation of gold nanoparticles using neoisoliquiritin in the extract of *Glycyrrhiza glabra* depends heavily on the pH of the solution. In an environment with low H^+ (increased pH) concentration, the readuction potential is very high. This process causes the concentration of H^+ in the solution to increase (decreased pH), leading to slowing down of the reduction process. At this time, the capping process of neoisoliquiritin occurs more strongly on the surface of the nanoparticles, helping to stabilize the nanoparticles and avoid agglomeration. Besides, bioactive compounds and some important metabolites in plants, such as quercetin, dopamine, gallic acid, tannic acid, ascorbic acid, *etc.* also show great potential for synthesizing environmentally friendly AuNPs for practical application in colorimetric sensors due to their strong reducing properties. Jayeoye *et al.* utilized the substantial reducing properties of flavonoid quercetin to produce AuNPs with high uniformity. In this development strategy, quercetin plays a role as both a reducing agent and a stabilizing agent to produce stable AuNPs at room temperature with Al^{3+} sensitive reaction ability used as a fluoride detection probe based on the complexation reaction between Al^{3+} and fluoride that changes the color of the AuNP solution.[59] In another study, Ariski *et al.* proposed a green synthesis method using Jeju Hallabong peel extract (HPE) as a reducing and stabilizing agent (Fig. 4b).[57] This process successfully produced small, highly uniform gold nanoparticles with an absorption wavelength of 517 nm. In addition, the study showed that the gold nanoparticles produced using HPE exhibited much lower cytotoxicity than the AuNPs synthesized by the chemical reduction method. The formation mechanism

 This journal is © The Royal Society of Chemistry 2025

Published on 02 maggio 2025. Downloaded on 14/02/2026 03:50:09.

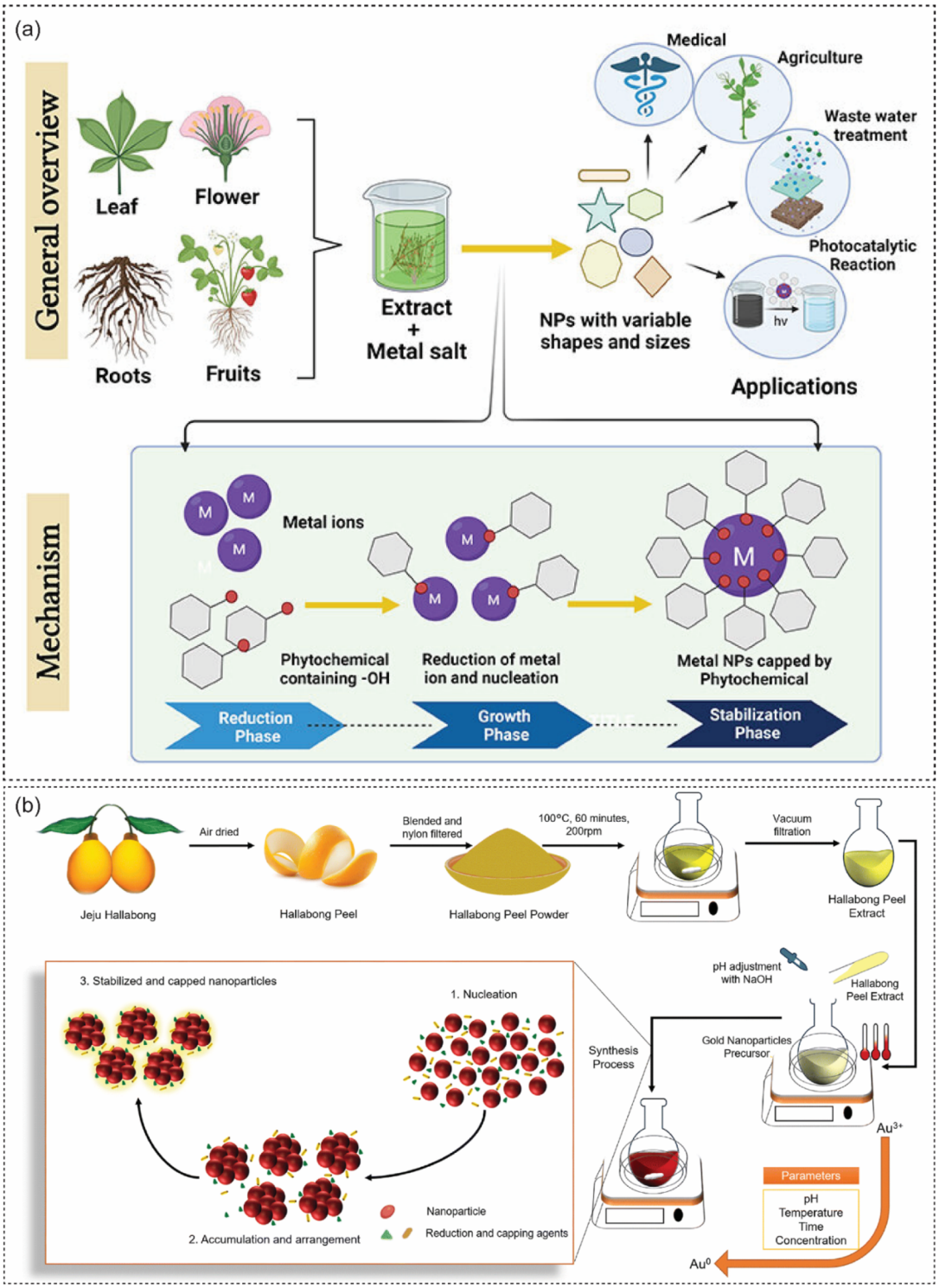

Fig. 4 (a) Schematic illustration of the general overview and mechanism involved in green synthesis of nanoparticles using extracted plants.[56] (b) Green synthesis of AuNPs from Jeju Hallabong extract as a reducing agent and capping agent.[57]

of AuNPs synthesized based on HPE, flavonoids, alkaloids, and phenolic compounds contained in the HPE extract that are reducing agents and stabilizers. The reducing agents are mainly phenolic compounds that provide electrons from the hydroxyl group. Meanwhile, flavonoid molecules act as a capping agent to limit the aggregation of AuNPs. Similar to chemical reduction, the morphology, size, and properties of gold nanoparticles from plant extracts depend primarily on the precursor ratio, temperature, and pH.[60] Reasonable control of these parameters helps to control gold nanoparticles to suit many applications.

Published on 02 maggio 2025. Downloaded on 14/02/2026 03:50:09.

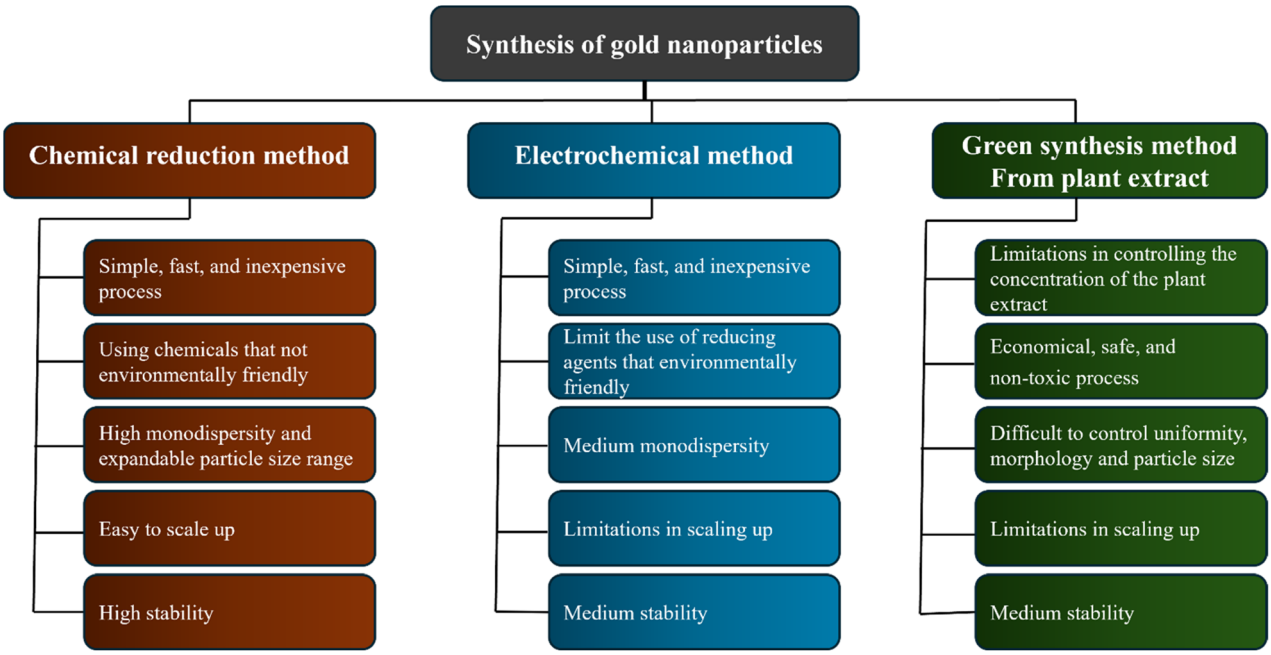

Fig. 5 Schematic summary of common features of AuNPs synthesis methods.[68–70]

Although the sources of reducing agents and stabilizers in plant extracts are abundant in quantity, it is difficult to control the content of substances in the extract, which leads to low reproducibility in synthesis batches. Besides green synthesis of gold nanoparticles from plant extracts, many other environmentally friendly synthesis methods, such as synthesis from fungi,[61] bacteria,[62] algae,[63] yeast,[64] and actinomycetes,[65] and the *in situ* chemical oxidative polymerization[66,67] methods, are also some of the strongly developed strategies in the trend of green synthesis of AuNPs. Fig. 5 depicts a summary review of some of the characteristics of the AuNP synthesis methods discussed in the paper.

Principle of colorimetric sensors for DNA detection based on gold nanoparticles

SPR-based colorimetric sensors

The plasmonic properties of AuNPs are one of the keys to the development strategies of colorimetric sensors for DNA detection. The sensitive variation of the plasmon frequency causes a color change in the AuNP solution, which can be observed by the naked eye. The particular intermolecular interactions between the target and surface modifiers can cause changes in particle aggregation or dispersion, shape, and size (etching, growth-mediated, and accumulation-based methods). Montaño-Priede *et al.* used computational simulations to describe the influence of morphology and size on extinction cross-section spectra (Fig. 6a).[71] The advantage of AuNPs compared to some other colorimetric methods is their simplicity and the ability to detect color based on the change in color of the material itself, which helps to limit the use of organic indicators that are often toxic. The dispersion-based color change method is commonly used, and this color change can originate from the direct interaction between DNA and AuNPs or through an intermediate. Tripathi *et al.* used the agglomeration effect of AuNPs to successfully detect *Mycobacterium tuberculosis* (MTB) DNA.[73] A simple color sensor was formed by adding PCR-amplified MTB DNA to AuNP solution in the presence of ethanol. Double-stranded DNA shows weaker interactions than single-stranded DNA due to the exposure of the negatively charged phosphate backbone.[74,75] The surface of AuNPs is covered with negatively charged citrate groups, which easily interact with the amine groups on nucleotide bases, making AuNPs more stable against agglomerating agents. Several other studies have also shown different levels of interaction between short-stranded DNA and long-stranded DNA with AuNPs. This can also be detected by the color change of the AuNP solution. Zhang *et al.* demonstrated the adsorption of DNA by gold nanoparticles using DNA adsorption kinetics and showed the influencing factors such as pH, salt concentration, and DNA concentration.[76] Although long-stranded DNA showed slower adsorption than oligo DNA fragments, after adsorption, it provided a more effective anti-aggregation ability for AuNPs. Besides the interaction with the target substance, AuNPs are susceptible to aggregation due to external factors such as pH, temperature, and ion concentration, which is the cause of false positive phenomena and limited selectivity of this method. Arumugam *et al.* used the redispersion of AuNPs instead of the agglomeration phenomenon to detect DNA using the colorimetric method to limit the influence of external factors on the accuracy of the colorimetric sensor.[77] Based on the principle of electrostatic attraction, a simple probe is created by adding carbon dots enriched with positively charged surface functional

 This journal is © The Royal Society of Chemistry 2025

Published on 02 maggio 2025. Downloaded on 14/02/2026 03:50:09.

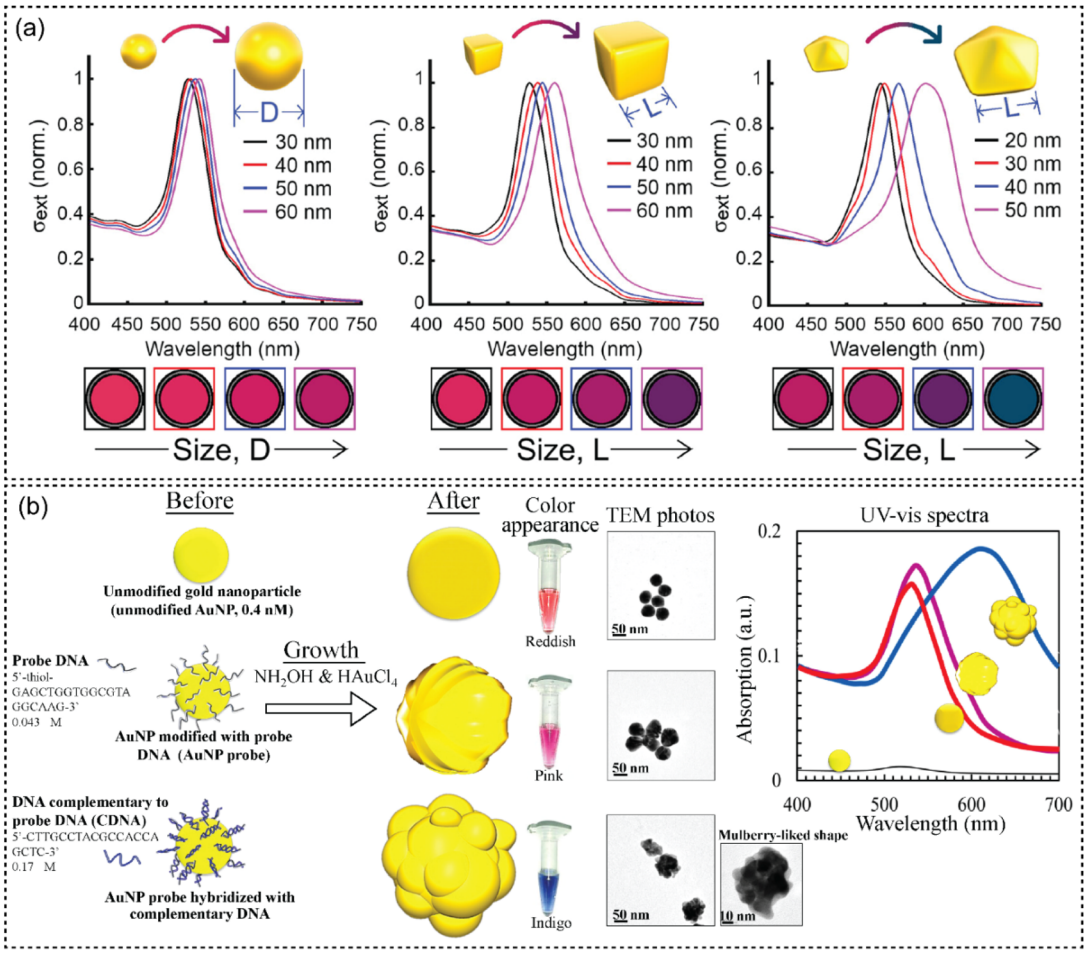

Fig. 6 (a) Calculated extinction cross-section spectra and the RGB colors derived from σ_{ext} of gold nanoparticles with different shapes and sizes.[71] (b) Schematic illustration of hybridization-mediated growth of the AuNP probe for detection of complementary DNA.[72]

groups into the AuNP solution at a suitable ratio, causing the aggregation of negatively charged AuNPs. For positive samples, the negatively charged DNAs interact with the carbon dots, reducing the aggregation of AuNPs, and the color of the solution changes from blue violet to red wine. This reaction achieves a detection limit of 1.7 nM in the linear range of 0.7–14 nM and is specific for both DNA and single-stranded DNA (ssDNA).

On the other hand, the method based on the etching of AuNPs showed much effectiveness in developing simple colorimetric sensors for application in DNA detection to overcome false positive results and increase selectivity. Creating additional labels for AuNPs in the aggregation method is also effective; however, this is very expensive and difficult to access in mass production of these sensors. Wang *et al.* reported a highly sensitive colorimetric method for telomerase detection in 15 HeLa cells using etched AuNRs.[78] The AuNRs are used as a visual signal reporter; for positive samples, the G-quadruplex/hemin DNAzymes are amplified by the catalytic hairpin assembly to convert 3,3′,5,5′-tetramethylbenzidine sulfate (TMB) to TMB in the oxidation state. The AuNRs are etched by TMB^{2+}, resulting in a change in the rod's aspect ratio, which the solution's color change can be visually detected. In contrast to etching, growth-mediated detection also has many advantages in detecting DNA with high sensitivity and selectivity. The morphology and size of gold nanoparticles during growth are greatly affected by the DNA modified on the surface of AuNPs.[79] Based on this principle, Fang *et al.* successfully developed a thiol-modified DNA functionalized AuNP probe to analyze concentration or distinguish DNA mismatch with a probe based on complementarity of DNA with the LOD reaching about 60 nM.[72] The grain growth mechanism due to the influence of the conductive target is proposed and depicted in Fig. 6b. With the advantages of sensitivity, simplicity, fast response time, and the ability to perform at room temperature, this method shows great promise in DNA detection.

Peroxidase activity-based colorimetric sensors

Metal nanoparticles (Au, Ag, Cu, Pt, Ni, *etc.*) are known for their excellent intrinsic catalytic ability for application in many fields, such as water treatment, sensors, and energy.[80] Gold nanoparticles with a (+) charged surface were first demonstrated to have peroxidase-like activity by Li *et al.* in 2010 with the ability to catalyze the color change of TMB from colorless to blue when exposed to H_2O_2.[81] In addition, the stability, biocompatibility,

Published on 02 maggio 2025. Downloaded on 14/02/2026 03:50:09.

and good binding ability with thiol and amine groups help AuNPs to be more widely applied in biosensors. Recently, colorimetric sensors based on peroxidase-like activity of AuNPs in DNA detection which greatly improved sensitivity and selectivity have been intensively studied. Wang *et al.* conducted a study demonstrating the influence of surface coating of gold nanoparticles on the peroxidase-like activity of AuNPs.[82] The activity of unmodified AuNPs was significantly higher than that of the control particles when coated with surface modifiers. Based on this property, AuNPs are applied to increase the sensitivity of colorimetric sensors when combined with other materials according to two main mechanisms: the expression of peroxidase-like activity and the inhibition of peroxidase-like activity. Peroxidase substrates such as TMB, 2,2′-azino bis (3-ethylbenzothiazoline-6-sulfonic acid) (ABTS), *o*-phenylenediamine (OPD) and diazoaminobenzene (DAB) are commonly used in colorimetric sensors with the common characteristic of easily changing color when oxidized by free radicals. Gold nanomaterials or hybrids of gold nanoparticles act as effective catalysts to convert H_2O_2 into $OH^{\bullet}$ radicals due to their highly positively charged surface. $OH^{\bullet}$ with strong oxidizing ability will change the color of peroxidase substrates. The target analytes are detected through two mechanisms: in the first case, direct interaction with gold nanoparticles causes a decrease in the surface area and catalytic capacity of AuNPs (indicator changes from colored to discolored – inhibition of peroxidase-like activity). In the second case, the analytes interact with the labels immobilized on the surface, releasing AuNPs, thereby increasing the catalytic activity of AuNPs (indicator changes from transparent to colored – peroxidase-like activity). Liu *et al.* presented a simple colorimetric method for rapid DNA detection based on the synergetic peroxidase-like activity of AuNPs assembled on the surface of iron-based metal–organic frameworks (Au@Fe-MIL-88).[83] Based on the adsorption properties of AuNPs towards DNAs causing inhibition of the peroxidase-like activity of the Au@Fe-MIL-88 hybrids, the addition of target DNA successfully counteracted this inhibition recognizing target DNA with the LOD reaching 11.4 nM in the range of 30–150 nM. The advantages of this method are its low cost, simplicity, and high efficiency, reducing false positives compared to the color detection method based on the agglomeration effect. Liu *et al.* used AuNPs as a peroxidase to convert TMB color *via* an oxidation reaction as a starting point in a label-free colorimetric sensor to detect *E. coli* bacteria.[84] A certain amount of aptamer was used to bind to the bacteria and the remaining part interacted with CTAB, reducing the inhibition of the catalytic activity of CTAB towards AuNPs, successfully obtaining the sensitivity of detection for *E. coli* bacteria reaching 5×10^3 CFU mL^{-1} visually and 75 CFU mL^{-1} using the UV-vis spectrum. With the advantages of quantitative and qualitative capabilities, a simple process, and no requirement for expensive equipment, this method has great potential in the on-site detection of microorganisms. In another study, Wang *et al.* developed a strategy using Janus Fe_3O_4–Au@Pt nanozymes to increase the sensitivity of the traditional colloidal gold-based lateral flow assay (LFA) in detecting H1N1 virus.[85] The sensor using enhanced-sensitive colorimetric nucleic acid lateral flow assay (NALFA) successfully improved the sensitivity of the LFA method with the LOD reaching 50 nM. Due to the high peroxidase-like activity of Fe_3O_4–Au@Pt NPs, the color values on test strips under catalyzed TMB to oxidize to the dark blue chelate (oxTMB) resulted in a 20-fold increase in color detection. The study provides an effective method for qualitative detection based on binding complementarily to DNA for identification of not only the H1N1 virus and also has the potential to expand the detection of many other viruses with rapid response time.

Applications in POCT for pathogenic bacteria and virus

During the COVID-19 pandemic, POCT have shown the importance of tools to rapidly detect harmful viruses, which helps to protect and improve healthcare for human beings.[86,87] Among existing techniques, AuNP-based colorimetric methods have been widely applied to detect bacteria and viruses, due to their simple and rapid measurements by the naked eye without the need for any complicated instruments.[88,89] A revolution in the development of gold nanoparticle-based biosensors has been achieved with a variety of different strategies aimed at detecting SARS-CoV-2, SARS-CoV-1, and MERS-CoV and lowly pathogenic CoVs such as colorimetric, electrochemical, ECL-based, LSPR colorimetric, SERS-based, and fluorescence-based sensing methods. The proof is the rapid introduction of commercial products using AuNP-based POCT kits such as the One Step Test for SARS-CoV-2 Antigen (Colloidal Gold-Getein Biotech, Inc./China), COVID-19 (SARS-CoV-2) Antigen Test Kit – Colloidal Gold (Anhui Deep Blue Medical Technology Co., Ltd – P.R.C), ScheBo® SARS-CoV-2 QuickTM Antigen (Colloidal Gold Method, ScheBo Biotech AG./Germany), and SARS-CoV-2 Antigen Rapid Test Cassette (Nasal Swab) (Surescreen Diagnostics Ltd/UK). In general, AuNP-based colorimetric sensors are usually employed for detection of amplified nucleic acid,[90,91] or non-amplified nucleic acid[85,92] by coupling with amplification techniques (LAMP, RCA, and PCR),[93,94] or incorporation into LFA.[95,96] For example, Ruang-areeate *et al.* suggested a novel distance-based paper device for detecting *Leishmania* among patients with HIV using combined SYBR safe and AuNP probe LAMP assays, and the LOD was 10^2 parasites per mL.[97] LAMP products were directly visualized and quantified using LAMP probe-streptavidin conjugated AuNPs for colorimetric precipitate induction. Besides, the combination of LAMP (DNA amplification) and lateral flow assays (LFA) (DNA detection) has been intensively developed for high sensitivity and specificity for visualizing nucleic acids of SARS-CoV-2 or *E. coli* O157:H7.[98,99] In another study, Biyani *et al.* developed an RICCA (RNA Isothermal Co-assisted and Coupled Amplification) reaction for lab-free testing of RNA viruses (Fig. 7a).[100] The colorimetric results were achieved after 5–10 min using a lateral flow dipstick where the biotinylated RICCA product hybridized with a digoxin-labeled DNA probe and complexed with a gold-labeled anti-digoxin antibody. In this way, AuNPs do not bind to the test line and hence there is no color where there were no DNA

 This journal is © The Royal Society of Chemistry 2025

Published on 02 maggio 2025. Downloaded on 14/02/2026 03:50:09.

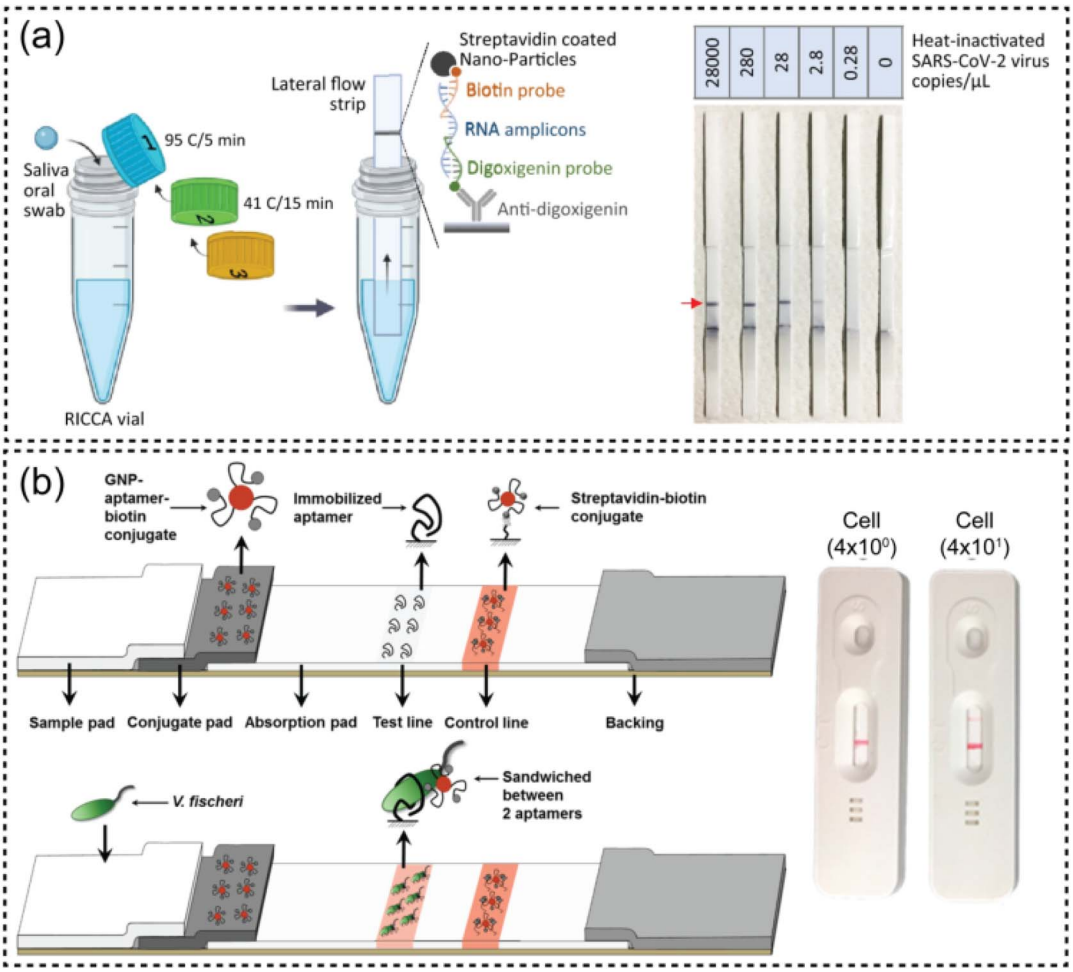

Fig. 7 (a) Direct saliva-to-RICCA-to-LF assay for the lab-free testing of SARS-CoV-2 virus.[100] (b) Schematic diagram of the principle for detection of the aptamer-based paper strip sensor.[101]

amplicons from RICCA assays. Kim *et al.* also developed paper-based colorimetric detection of target DNA that employs a radial flow assay according to the Au-probe labeling strategy.[102] In detail, RCA amplicons were hybridized with a DNA-probe on 20 nm AuNPs to form a large complex, resulting in a red circular colorimetric pattern on a nitrocellulose paper chip. In the presence of DNA, the circular area was extended as the concentration of the target DNA increased.

On the other hand, a AuNP-based colorimetric approach was also effectively employed to rapidly detect other analytes such as proteins, lipopolysaccharides, or intact cells from common pathogens causing serious diseases such as *Salmonella typhimurium*,[103–105] *Staphylococcus aureus*,[106] *Escherichia coli* O157:H7,[107,108] *etc.* In general, these approaches have used sandwich-type immunoreactions that were performed on the LFA, and they are based on using AuNPs as a label for reporting antibodies. Recently, Shin *et al.* introduced a paper strip sensor for rapid detection of *Vibrio fischeri* based on aptamer sandwich assay (Fig. 7b).[101] With the use of aptamer-conjugated gold nanoparticle probes in a paper strip, the colorimetric response of a paper sensor was as low as 4×10^1 CFU mL^{-1} of the target cell, and it displayed a significant ability to detect and discriminate *Vibrio fischeri* from other bacterial species. Similarly, Mondal *et al.* also developed a portable biosensor based on the sandwich type format using dual aptamer-functionalized 23 nm AuNP-based LFA kits for real-time analysis of *Mammaliicoccus* sp. and *Pseudomonas* sp. within 5 min.[109] The colorimetric detection was confirmed by the changes in the color of the solution, where the sample turned colorless when AuNP-thiol modified aptamers bound to the target. A comparison of pathogen detection test platforms based on AuNPs is presented in Table 1.

In conclusion, the AuNP-based colorimetric method is still a great potential platform for the robust, cost-effective, sensitive, and specific identification of bacterial and viral pathogens. Nevertheless, further advanced POCT is required to allow such a higher sensitivity with low-volume analysis by moving from colloidal AuNPs to bimetallic (Pt/Au, Ag/Au, or Au/Pd).[112,113] In addition to inheriting optical, electrical, and catalytic properties from single components, bimetallic materials possess many other unique properties arising from the synergistic interactions of different metal nanostructures.[114,115] Specifically, in colorimetric sensors, bimetallic nanoparticles have been shown to have much higher sensitivity than single-component

Published on 02 maggio 2025. Downloaded on 14/02/2026 03:50:09.

Table 1 Comparison of pathogen detection test platforms based on AuNPs

Test platform	Biorecognition element types	Pathogen	Target molecule	LOD	Analysis time	Reference
LAMP-LFA	Antibody-functionalized gold nanoparticles	SARS-CoV-2 and influenza-A	Nucleic acid	—	30 min	Akalın *et al.*, 2023 (ref. 110)
LAMP-LFA	Antibody-functionalized gold nanoparticles	SARS-CoV-2	Nucleic acid	3.9×10^3 RNA copies per mL	15 min	Agarwal *et al.*, 2022 (ref. 111)
RCA-LFA	AuNP-probe	—	DNA	14.7 nM	—	Kim *et al.*, 2023 (ref. 102)
RICCA-LFA	AuNP-probe	*E. coli* cells SARS-CoV-2	RNA	8 CFU μL^{-1} and 1740 copies per μL	15–30 min	Biyani *et al.*, 2021 (ref. 100)
AuNP-LAMP (color & precipitate)	Probe-streptavidin conjugated AuNPs	*Leishmania*	cDNA	102 parasites per mL (0.0147 ng μL^{-1})	15 min	Ruang-areerate *et al.*, 2022 (ref. 97)
Au-on-Au tip sensors	DNA-conjugated AuNPs	*Salmonella typhimurium*	Protein	3.2×10^3 CFU mL^{-1}	1 h	Li *et al.*, 2023 (ref. 104)
Colorimetric biosensor	Antibody-functionalized gold nanoparticles	*Salmonella typhimurium*	Cell	1 CFU mL^{-1}	15 min	Anzevino *et al.*, 2024 (ref. 103)
All-in-one portable biosensor	Aptamer-functionalized gold nanoparticles	*Mammaliicoccus* sp. and *Pseudomonas* sp.	Cell and cDNA	1.5×10^4 CFU mL^{-1} and 1.5×10^3 CFU mL^{-1}	—	Modal *et al.*, 2024 (ref. 109)
Paper strip sensor	DNA aptamer probes	*Vibrio fischeri*	Cell	4×10^1 CFU mL^{-1}	—	Shin *et al.*, 2018 (ref. 101)

materials when used directly as biochromic probes. In addition, the LSPR properties can also be controlled more flexibly by adjusting the component ratio. This provides many advantages and diversity in the design of biosensor probes. On the other hand, the synergistic effect also creates many unique catalytic properties of nanozymes when two metal centers interact with each other. The difference in electronegativity and redox potential of the two metals is the cause of the formation of new enzymatic activity or enhancement of existing enzymatic activity. Many recently published studies demonstrate the development trend of bimetallic nanomaterials as an alternative to single-component AuNPs.[66,116]

Conclusions

This review provides a comprehensive overview of the potential of AuNPs in colorimetric sensors for DNA detection. The solutions improve the sensitivity and selectivity that have hindered the development of colorimetric sensors compared with other types. The continuous development of AuNPs in many fields is convincing evidence of the diverse application potential of this material. Methods for synthesizing and controlling the properties of AuNPs are constantly being improved to suit many fields requiring high stability, such as sensors. Based on the SPR effect of AuNPs to produce sensitive color changes, the probe has been applied to the development of many types of colorimetric sensors. The limitations of poor sensitivity and specificity of colorimetric sensors are gradually overcome by using a combination of labels or based on the specificity of DNA. In this study, we focus on describing standard synthesis methods of AuNPs for colorimetric sensing and highlight recent advances in the synthesis and property control of AuNPs. The development strategies of AuNP-based colorimetric sensors are also presented in detail to provide an overview of the progress achieved, as well as the advantages and challenges.

Overall, simple sensors that allow rapid on-site target detection gradually replace bulky sensor systems and are a common development trend in the current sensor field. The AuNP-based method is still a suitable and promising choice for colorimetric sensors applied in the detection of biomolecules. Accuracy and sensitivity are no longer too big obstacles in the development and application of colorimetric sensors. However, some limitations remain to be overcome for further improvement:

- Even tiny inconsistencies in reaction parameters such as temperature, pH, reaction time, and concentration of reducing agents can lead to significant changes in the properties of the resulting AuNPs. To ensure the reproducibility and consistency of AuNPs, standard protocols for manipulating AuNP properties need to be established. Integrating the AuNP synthesis process with current emerging technologies such as artificial intelligence (AI) and automated systems can accelerate the synthesis process. An AI-powered forecasting system can predict possible conditions for AuNP synthesis with specific properties at low cost, while automated systems have the potential to enable high-throughput synthesis with minimal human error, enhanced precision, and reduced variability.
- AuNPs are versatile types of nanomaterial that possess diverse functionalities; however, there are limited studies that attempt to integrate multiple functions of AuNPs into a single

 This journal is © The Royal Society of Chemistry 2025

platform. Firstly, various mechanisms of AuNPs for generating signal outputs can be employed for fabrication of multiple-mode sensors. Future studies can consider integrating the SPR effect, peroxidase-like activity, fluorescence quenching/enhancement properties, Raman signal enhancement (SERS), and electrochemical signal amplification into a single platform. Secondly, multifunctional sensors can be fabricated by employing the photothermal effect for the heating process and magnetic hybridization for sample separation, further expanding the potential applications of AuNPs.

Data availability

Data sharing is not applicable to this article as no new data were created or analyzed in this study.

Conflicts of interest

There are no conflicts to declare.

Acknowledgements

This research received no external funding. The authors express their sincere gratitude to Tra Vinh University for generous support in this work. Also, the authors would like to gratefully acknowledge the Nguyen Tat Thanh University for support in this work.

Notes and references

1 M. A. Abedalwafa, Y. Li, C. Ni and L. Wang, *Anal. Methods*, 2019, **11**, 2836–2854.
2 Z. Chen, Z. Zhang, J. Qi, J. You, J. Ma and L. Chen, *J. Hazard. Mater.*, 2023, **441**, 129889.
3 S. Hussain, S. Majumder, U. C. De, D. Bhattacharjee, S. Hussain and S. A. Hussain, *Interactions*, 2024, **245**, 1–21.
4 P. Yan, X. Zheng, S. Liu, Y. Dong, T. Fu, Z. Tian and Y. Wu, *ACS Sens.*, 2023, **8**, 133–140.
5 Y. Qi, Y. Chen, J. He and F. Xiu, *Microchem. J.*, 2020, **159**, 105546.
6 W. Zhang, J. Song, H. Zheng and X. Xu, *Chem. Commun.*, 2022, **58**, 8666–8669.
7 V. Sekar, A. Santhanam and P. Arunkumar, *J. Water Process Eng.*, 2024, **59**, 105102.
8 V. X. T. Zhao, T. I. Wong, X. T. Zheng, Y. N. Tan and X. Zhou, *Mater. Sci. Energy Technol.*, 2020, **3**, 237–249.
9 L. Chen, W. Lu, X. Wang and L. Chen, *Sens. Actuators, B*, 2013, **182**, 482–488.
10 B. Yin, W. Zheng, M. Dong, W. Yu, Y. Chen, S. W. Joo and X. Jiang, *Analyst*, 2017, **142**, 2954–2960.
11 G. Topcu, T. Guner, E. Inci and M. M. Demir, *Sens. Actuators, A*, 2019, **295**, 503–511.
12 M. P. Mcoyi, K. T. Mpofu, M. Sekhwama and P. Mthunzi-Kufa, *Plasmonics*, 2024, **2024**, 1–40.
13 J. N. Anker, W. P. Hall, O. Lyandres, N. C. Shah, J. Zhao and R. P. Van Duyne, *Nanosci. Technol.*, 2009, **7**, 308–319.
14 A. Karnwal, R. S. Kumar Sachan, I. Devgon, J. Devgon, G. Pant, M. Panchpuri, A. Ahmad, M. B. Alshammari, K. Hossain and G. Kumar, *ACS Omega*, 2024, **9**, 29966–29982.
15 T. Ferreira-Gonçalves, D. Nunes, E. Fortunato, R. Martins, A. P. de Almeida, L. Carvalho, D. Ferreira, J. Catarino, P. Faísca, H. A. Ferreira, M. M. Gaspar, J. M. P. Coelho and C. P. Reis, *Int. J. Pharm.*, 2024, **650**, 123659.
16 Y. Ghafari, A. Asefnejad and D. O. Ogbemudia, *Sci. Hypotheses*, 2024, **1**, 21–35.
17 E. G. Wrigglesworth and J. H. Johnston, *Nanoscale Adv.*, 2021, **3**, 3530–3536.
18 M. Zhang, S. Shao, H. Yue, X. Wang, W. Zhang, F. Chen, L. Zheng, J. Xing and Y. Qin, *Int. J. Nanomed.*, 2021, **16**, 6067–6094.
19 R. J. Kadhim, E. H. Karsh, Z. J. Taqi and M. S. Jabir, *Mater. Today Proc.*, 2021, **42**, 3041–3045.
20 T. Bohdanovych, P. Kuzema, V. Anishchenko, V. Duplij, M. Kharchuk, V. Lyzhniuk, A. Shakhovsky and N. Matvieieva, *Biol. Open*, 2025, **14**, bio061739.
21 S. Behera, G. Rana, S. Satapathy, M. Mohanty, S. Pradhan, M. K. Panda, R. Ningthoujam, B. N. Hazarika and Y. D. Singh, *Sens. Int.*, 2020, **1**, 100054.
22 M. Tavakkoli Yaraki and Y. N. Tan, *Sens. Int.*, 2020, **1**, 100049.
23 G. A. Naikoo, F. Arshad, I. U. Hassan, T. Awan, H. Salim, M. Z. Pedram, W. Ahmed, V. Patel, A. S. Karakoti and A. Vinu, *Bioeng. Transl. Med.*, 2022, **7**, e10305.
24 Y. Y. Cheng, Z. Chen, X. Cao, T. D. Ross, T. G. Falbel, B. M. Burton and O. S. Venturelli, *Nat. Commun.*, 2023, **14**, 1–11.
25 J. Kimling, M. Maier, B. Okenve, V. Kotaidis, H. Ballot and A. Plech, *J. Phys. Chem. B*, 2006, **110**, 15700–15707.
26 L. I. M. Silva, A. Pérez-Gramatges, D. G. Larrude, J. M. S. Almeida, R. Q. Aucélio and A. R. da Silva, *Colloids Surf., A*, 2021, **614**, 126174.
27 C. Ziegler and A. Eychmüller, *J. Phys. Chem. C*, 2011, **115**, 4502–4506.
28 L. Malassis, R. Dreyfus, R. J. Murphy, L. A. Hough, B. Donnio and C. B. Murray, *RSC Adv.*, 2016, **6**, 33092–33100.
29 M. H. Moosavy, M. de la Guardia, A. Mokhtarzadeh, S. A. Khatibi, N. Hosseinzadeh and N. Hajipour, *Sci. Rep.*, 2023, **13**, 1–15.
30 O. J. H. Chai and J. Xie, *J. Phys. Chem. Lett.*, 2024, **15**, 5137–5142.
31 Y. Z. Wu, Y. Y. Tsai, L. Sen Chang and Y. J. Chen, *Pharmaceuticals*, 2021, **14**, 1071.
32 S. Y. Park, R. Sivakumar and N. Y. Lee, *Biosensors*, 2024, **14**, 284.
33 S. Yoo, G. Youn, H. Lee, J. S. Kwon, Y. Lee and S. Lee, *Bull. Korean Chem. Soc.*, 2023, **44**, 648–652.
34 S. Yoo, D. H. Nam, T. I. Singh, G. Leem and S. Lee, *Nano Convergence*, 2022, **9**, 1–9.
35 Y. Ding, P. J. J. Huang, M. Zandieh, J. Wang and J. Liu, *Langmuir*, 2023, **39**, 256–264.

Published on 02 maggio 2025. Downloaded on 14/02/2026 03:50:09.

Published on 02 maggio 2025. Downloaded on 14/02/2026 03:50:09.

36 M. R. Langille, M. L. Personick, J. Zhang and C. A. Mirkin, *J. Am. Chem. Soc.*, 2012, **134**, 14542–14554.
37 M. L. Personick, M. R. Langille, J. Zhang, N. Harris, G. C. Schatz and C. A. Mirkin, *J. Am. Chem. Soc.*, 2011, **133**, 6170–6173.
38 S. Yazdani, A. Daneshkhah, A. Diwate, H. Patel, J. Smith, O. Reul, R. Cheng, A. Izadian and A. R. Hajrasouliha, *ACS Omega*, 2021, **6**, 16847–16853.
39 G. Mountrichas, S. Pispas and E. I. Kamitsos, *J. Phys. Chem. C*, 2014, **118**, 22754–22759.
40 T. Gholami, H. Seifi, E. A. Dawi, M. Pirsaheb, S. Seifi, A. M. Aljeboree, A. H. M. Hamoody, U. S. Altimari, M. Ahmed Abass and M. Salavati-Niasari, *Mater. Sci. Eng., B*, 2024, **304**, 117370.
41 M. He, X. Liu, B. Liu and J. Yang, *J. Colloid Interface Sci.*, 2019, **537**, 414–421.
42 R. Herizchi, E. Abbasi, M. Milani and A. Akbarzadeh, *Artif. Cells, Nanomed., Biotechnol.*, 2016, **44**, 596–602.
43 Y. Y. Yu, S. S. Chang, C. L. Lee and C. R. C. Wang, *J. Phys. Chem. B*, 1997, **101**, 6661–6664.
44 X. Y. Liu, C. Y. Cui, Y. W. Cheng, H. Y. Ma and D. Liu, *Int. J. Miner. Metall. Mater.*, 2013, **20**, 486–492.
45 P. G. Haro-González, D. S. Ramírez-Rico and E. R. Larios-Durán, *Int. J. Electrochem. Sci.*, 2019, **14**, 9704–9710.
46 P. Maguire, D. Rutherford, M. Macias-Montero, C. Mahony, C. Kelsey, M. Tweedie, F. Pérez-Martin, H. McQuaid, D. Diver and D. Mariotti, *Nano Lett.*, 2017, **17**, 1336–1343.
47 C. Xu, S. Chaudhuri, J. Held, H. P. Andaraarachchi, G. C. Schatz and U. R. Kortshagen, *J. Phys. Chem. Lett.*, 2023, **14**, 9960–9968.
48 J. H. Nam, G. Nayak, S. Exarhos, C. M. Mueller, D. Xu, G. C. Schatz and P. J. Bruggeman, *Chem. Sci.*, 2024, **15**, 11643–11656.
49 J. H. Nam and P. Bruggeman, *Plasma Processes Polym.*, 2025, **22**, 2400140.
50 Y. Shang, C. Min, J. Hu, T. Wang, H. Liu and Y. Hu, *Solid State Sci.*, 2013, **15**, 17–23.
51 B. Azemoodeh Afshar, A. Jafari, M. Maqsood Golzan and R. Naderali, *Results Opt.*, 2023, **12**, 100462.
52 K. Okitsu, A. Yue, S. Tanabe, H. Matsumoto and Y. Yobiko, *Langmuir*, 2001, **17**, 7717–7720.
53 S. Eustis, H. Y. Hsu and M. A. El-Sayed, *J. Phys. Chem. B*, 2005, **109**, 4811–4815.
54 P. B. Santhosh, J. Genova and H. Chamati, *Chemistry*, 2022, **4**, 345–369.
55 S. Ahmed, Annu, S. Ikram and S. Yudha, *J. Photochem. Photobiol., B*, 2016, **161**, 141–153.
56 H. Singh, M. F. Desimone, S. Pandya, S. Jasani, N. George, M. Adnan, A. Aldarhami, A. S. Bazaid and S. A. Alderhami, *Int. J. Nanomed.*, 2023, **18**, 4727–4750.
57 R. T. Ariski, K. K. Lee, Y. Kim and C. S. Lee, *RSC Adv.*, 2024, **14**, 14582–14592.
58 A. O. E. Eltahir, K. L. Lategan, O. M. David, E. J. Pool, R. C. Luckay and A. A. Hussein, *J. Funct. Biomater.*, 2024, **15**, 95.
59 T. J. Jayeoye, R. Panghiyangani, S. Singh and N. Muangsin, *Nanomaterials*, 2024, **14**, 1967.
60 S. Bhaskaran, N. Sharma, P. Tiwari, S. R. Singh and S. V. Sahi, *Sci. Rep.*, 2019, **9**, 1–9.
61 Z. Molnár, V. Bódai, G. Szakacs, B. Erdélyi, Z. Fogarassy, G. Sáfrán, T. Varga, Z. Kónya, E. Tóth-Szeles, R. Szucs and I. Lagzi, *Sci. Rep.*, 2018, **8**, 1–12.
62 C. Aarti, A. Khusro, P. Agastian, P. Kuppusamy and D. A. Al Farraj, *J. King Saud Univ., Sci.*, 2022, **34**, 101974.
63 M. Ramakrishna, D. Rajesh Babu, R. M. Gengan, S. Chandra and G. Nageswara Rao, *J. Nanostruct. Chem.*, 2016, **6**, 1–13.
64 X. Zhang, Y. Qu, W. Shen, J. Wang, H. Li, Z. Zhang, S. Li and J. Zhou, *Colloids Surf., A*, 2016, **497**, 280–285.
65 S. Aati, H. Y. Aati, A. A. Hamed, S. El-Shamy, S. H. Aati, U. R. Abdelmohsen, G. Bringmann, M. N. Taha, H. M. Hassan and H. S. Bahr, *RSC Adv.*, 2025, **15**, 3954–3968.
66 Y. Zhang, B. Zhang, Z. Guo, S. Lu, Y. Li and R. Zhang, *Anal. Chim. Acta*, 2025, **1341**, 343685.
67 T. J. Jayeoye and N. Muangsin, *Mater. Today Sustainability*, 2024, **27**, 100829.
68 C. Daruich De Souza, B. Ribeiro Nogueira and M. E. C. M. Rostelato, *J. Alloys Compd.*, 2019, **798**, 714–740.
69 I. Saldan, O. Dobrovetska, L. Sus, O. Makota, O. Pereviznyk, O. Kuntyi and O. Reshetnyak, *J. Solid State Electrochem.*, 2017, **22**, 637–656.
70 J. Qiao and L. Qi, *Talanta*, 2021, **223**, 121396.
71 J. L. Montaño-Priede, M. Sanromán-Iglesias, N. Zabala, M. Grzelczak and J. Aizpurua, *ACS Sens.*, 2023, **8**, 1827–1834.
72 W. F. Fang, W. J. Chen and J. T. Yang, *Sens. Actuators, B*, 2014, **192**, 77–82.
73 A. Tripathi, R. Jain and P. Dandekar, *Anal. Methods*, 2023, **15**, 2497–2504.
74 L. Yu and N. Li, *Chemosensors*, 2019, **7**, 53.
75 H. Li and L. J. Rothberg, *J. Am. Chem. Soc.*, 2004, **126**, 10958–10961.
76 X. Zhang, M. R. Servos and J. Liu, *Langmuir*, 2012, **28**, 3896–3902.
77 S. S. Arumugam, A. W. Varghese, S. Suresh Nair and N. Y. Lee, *Anal. Methods*, 2023, **15**, 5793–5802.
78 D. Wang, R. Guo, Y. Wei, Y. Zhang, X. Zhao and Z. Xu, *Biosens. Bioelectron.*, 2018, **122**, 247–253.
79 Z. Wang, J. Zhang, J. M. Ekman, P. J. A. Kenis and Y. Lu, *Nano Lett.*, 2010, **10**, 1886–1891.
80 X. Liu, D. Huang, C. Lai, L. Qin, G. Zeng, P. Xu, B. Li, H. Yi and M. Zhang, *Small*, 2019, **15**, 1900133.
81 Y. Jv, B. Li and R. Cao, *Chem. Commun.*, 2010, **46**, 8017–8019.
82 S. Wang, W. Chen, A. L. Liu, L. Hong, H. H. Deng and X. H. Lin, *ChemPhysChem*, 2012, **13**, 1199–1204.
83 Y. L. Liu, W. L. Fu, C. M. Li, C. Z. Huang and Y. F. Li, *Anal. Chim. Acta*, 2015, **861**, 55–61.
84 M. Liu, F. Zhang, S. Dou, J. Sun, F. Vriesekoop, F. Li, Y. Guo and X. Sun, *Anal. Methods*, 2023, **15**, 1661–1667.
85 K. Wang, D. Yu, X. Liang, W. Lu, X. Jiang, K. Tashpulatov, J. Zeng and C. Y. Wen, *Microchem. J.*, 2024, **204**, 111104.

 This journal is © The Royal Society of Chemistry 2025

Published on 02 maggio 2025. Downloaded on 14/02/2026 03:50:09.

86 Y. Joung, K. Kim, J. E. An, S. Park, Q. Yu, M. Lu, J. Chen, S. W. Joo and J. Choo, *Trends Biotechnol.*, 2024, **43**, 1048–1061.
87 M. Xiao, F. Tian, X. Liu, Q. Zhou, J. Pan, Z. Luo, M. Yang and C. Yi, *Adv. Sci.*, 2022, **9**, 2105904.
88 M. Abdolhosseini, F. Zandsalimi, F. S. Moghaddam and G. Tavoosidana, *J. Virol. Methods*, 2022, **301**, 114461.
89 Y. Choi, J. H. Hwang and S. Y. Lee, *Small Methods*, 2018, **2**, 1700351.
90 S. Kooti, R. Abiri, S. Kadivarian, S. Khazayel, P. Mohajeri, S. Atashi, F. Yari, H. Ahmadpour and A. Alvandi, *Sens. Bio-Sens. Res.*, 2022, **38**, 100543.
91 M. Djisalov, L. Janjušević, V. Léguillier, L. Šašić Zorić, C. Farre, J. Anba-Mondoloni, J. Vidic and I. Gadjanski, *Sci. Rep.*, 2024, **14**, 1–10.
92 L. Tessaro, A. Aquino, A. P. A. de Carvalho and C. A. Conte-Junior, *Sens. Actuators Rep.*, 2021, **3**, 100060.
93 M. Elumalai, A. Ipatov, J. Carvalho, J. Guerreiro and M. Prado, *Anal. Bioanal. Chem.*, 2022, **414**, 5239–5253.
94 G. Alhamid, H. Tombuloglu, H. A. BenRashed, M. A. Almessiere and A. A. Rabaan, *Microchim. Acta*, 2024, **191**, 1–11.
95 H. Sohrabi, M. R. Majidi, M. Fakhraei, A. Jahanban-Esfahlan, M. Hejazi, F. Oroojalian, B. Baradaran, M. Tohidast, M. de la Guardia and A. Mokhtarzadeh, *Talanta*, 2022, **243**, 123330.
96 H. Sohrabi, M. R. Majidi, P. Khaki, A. Jahanban-Esfahlan, M. de la Guardia and A. Mokhtarzadeh, *Compr. Rev. Food Sci. Food Saf.*, 2022, **21**, 1868–1912.
97 T. Ruang-areerate, N. Saengsawang, P. Ruang-areerate, N. Ratnarathorn, T. Thita, S. Leelayoova, S. Siripattanapipong, K. Choowongkomon and W. Dungchai, *Sci. Rep.*, 2022, **12**, 1–14.
98 J. H. Kim and S. W. Oh, *J. Food Sci. Technol.*, 2019, **56**, 2576–2583.
99 Y. Wen, Y. Tan, L. Zhao, X. Lv, L. Lin, D. Liang and L. Wang, *Microchem. J.*, 2022, **178**, 107348.
100 R. Biyani, K. Sharma, K. Kojima, M. Biyani, V. Sharma, T. Kumawat, K. M. Juma, I. Yanagihara, S. Fujiwara, E. Kodama, Y. Takamura, M. Takagi, K. Yasukawa and M. Biyani, *Sci. Rep.*, 2021, **11**, 1–13.
101 W. R. Shin, S. S. Sekhon, S. K. Rhee, J. H. Ko, J. Y. Ahn, J. Min and Y. H. Kim, *ACS Comb. Sci.*, 2018, **20**, 261–268.
102 T. Y. Kim, S. Kim, J. H. Jung and M. A. Woo, *Biochip J.*, 2023, **17**, 263–273.
103 M. Anzevino, D. Marra, A. Fulgione, A. Giarra, D. Nava, L. Biondi, F. Capuano, V. Iannotti, B. Della Ventura and R. Velotta, *ACS Appl. Nano Mater.*, 2024, **7**, 21048–21056.
104 J. Li, S. Khan, J. Gu, C. D. M. Filipe, T. F. Didar and Y. Li, *Angew. Chem., Int. Ed.*, 2023, **62**, e202300828.
105 Q. Chen, R. Gao and L. Jia, *Talanta*, 2021, **221**, 121476.
106 M. Sanromán-Iglesias, V. Garrido, Y. Gil-Ramírez, J. Aizpurua, M. Grzelczak and M. J. Grilló, *Sens. Actuators, B*, 2021, **349**, 130780.
107 J. Fu, Y. Zhou, X. Huang, W. Zhang, Y. Wu, H. Fang, C. Zhang and Y. Xiong, *J. Agric. Food Chem.*, 2020, **68**, 1118–1125.
108 T. Jiang, Y. Song, T. Wei, H. Li, D. Du, M. J. Zhu and Y. Lin, *Biosens. Bioelectron.*, 2016, **77**, 687–694.
109 R. Mondal, J. Chakraborty, P. Dam, S. Shaw, D. Gangopadhyay, Y. N. Ertas and A. K. Mandal, *ACS Appl. Bio Mater.*, 2024, **7**, 5740–5753.
110 P. Akalın and A. Yazgan-Karataş, *MethodsX*, 2023, **11**, 102372.
111 S. Agarwal, C. Warmt, J. Henkel, L. Schrick, A. Nitsche and F. F. Bier, *Anal. Bioanal. Chem.*, 2022, **414**, 3177–3186.
112 H. Peng and I. A. Chen, *ACS Nano*, 2019, **13**, 1244–1252.
113 L. Ferretti, C. Wymant, M. Kendall, L. Zhao, A. Nurtay, L. Abeler-Dörner, M. Parker, D. Bonsall and C. Fraser, *Science*, 2020, **368**, 83.
114 A. I. Ribeiro, A. M. Dias and A. Zille, *ACS Appl. Nano Mater.*, 2022, **5**, 3030–3064.
115 X. Liu, X. Liang, J. Yu, K. Xu, J. W. Shen, W. Duan and J. Zeng, *TrAC, Trends Anal. Chem.*, 2023, **169**, 117386.
116 Y. Zhao, M. Guan, F. Mi, Y. Zhang, P. Geng, S. Zhang, H. Song and G. Chen, *Mikrochim. Acta*, 2025, **192**, 83.